

# Effect of Rheology on Gel Placement

R.S. Seright, SPE, New Mexico Petroleum Recovery Research Center

**Summary.** This study investigates whether rheology can be exploited to eliminate the need for zone isolation during gel placement. Eight different rheological models were used to represent the properties of existing non-Newtonian gelling agents. Gel placement was examined in linear and radial parallel corefloods and in fractured and unfractured injection wells. The analysis indicates that, compared with water-like gelling agents, existing non-Newtonian gelling agents will not reduce the need for zone isolation during gel placement in radial-flow systems.

## Introduction

Near-wellbore gel treatments in injection wells are intended to block fractures or high-permeability zones so that fluids injected after the gel treatment are more likely to enter and displace oil from other strata.

In most cases, when gelling agents are injected to alter flow profiles in a well, zones are not isolated and the chemicals have access to all open intervals. Of course, much of the gelant formulation will enter fractures and/or high-permeability streaks. Some of this fluid, however, can enter and damage less-permeable, hydrocarbon-bearing strata. Recent investigations<sup>1-3</sup> focused on how flow profiles are modified by unrestricted injection of Newtonian gelling agents. These studies indicate that zone isolation is much more likely to be needed during gel placement in unfractured wells than in fractured wells. Productive zones in unfractured wells can be seriously damaged if zones are not isolated during gel placement.

These studies do not suggest that zone isolation is a cure-all during gel treatments. Clearly, mechanical isolation of zones is not feasible in many (perhaps most) cases. Also, zone isolation is of little benefit if extensive crossflow can occur between layers or if flow behind pipe can occur. Rather, our analyses are intended to aid in assessing how and where gel treatments are best applied.

The fundamental question addressed in this paper asks whether gelling-agent rheology can be exploited to eliminate the need for zone isolation during gel placement.

Numerical methods are used to examine how flow profiles are modified with non-Newtonian gelling agents. First, rheological models are summarized for flow of existing polymeric fluids in porous media. Then, these models are applied to calculate the degree of penetration during unrestricted injection of gelling agent into various two-layer systems. These systems include linear and radial parallel corefloods and fractured and unfractured injection wells. In this paper, the terms "gelling agent" and "gelant" refer to the liquid formulation before gelation.

## Rheological Models for Existing Polymeric Fluids

Eight different rheological models were used to represent the properties of existing non-Newtonian gelling agents. Five shear-thinning models and three shear-thickening models are included. Figs. 1 through 5 illustrate the rheological behavior predicted by five of the models in 100- and 1,000-md rock. The other three models are illustrated in Ref. 4.

**Power-Law Model.** A number of power-law models have been proposed for flow of non-Newtonian fluids in porous media.<sup>5-9</sup> In these models, the relation between the fluid resistance factor,  $F_r$ , and superficial fluid velocity,  $u$ , is given by

$$F_r = Hu^{n-1}, \dots \dots \dots (1)$$

$$\text{where } H = c_1(3 + 1/n)^n(k/\phi)^{(1-n)/2}, \dots \dots \dots (2)$$

Here,  $F_r$  = water mobility divided by gelant mobility,  $n$  = power-law exponent from viscosity-vs.-shear-rate data,  $k$  = effective permeability to water, and  $\phi$  = effective aqueous-phase porosity. The principal difference among the various power-law models occurs

in the value of  $c_1$ . The particular power-law model chosen for this work was Teeuw and Hesselink's.<sup>8</sup> In this model,

$$c_1 = I/(\mu_w 8^n \sqrt{2}), \dots \dots \dots (3)$$

where  $I$  = consistency index from viscosity-vs.-shear-rate data and  $\mu_w$  = water viscosity.

Fig. 1 illustrates the rheology predicted by the power-law model for low and high polymer concentrations in 100- and 1,000-md rock. The plots are based on the power-law portion of experimental data for 200- and 2,400-ppm xanthan solutions reported by Chauveteau<sup>10</sup> and Chauveteau and Zaitoun.<sup>11</sup> Two points in Fig. 1 should be noted. First, for each polymer concentration, the 100-md curve may be obtained by simply shifting the 1,000-md curve to the left by a factor of  $\sqrt{1,000/100}$ . This feature is common to six of the eight rheological models described in this section. (The two exceptions are the Willhite empirical power-law model and the Chauveteau depletion-layer model.) The second important observation is that the power-law model is not applicable at high fluid velocities because it predicts resistance factors less than unity. Resistance factors of aqueous solutions of polymers and gelants should be greater than unity. Power-law predictions can also be incorrect at very low fluid velocities.<sup>12</sup>

**Carreau Model.** The Carreau model<sup>13</sup> often provides the most accurate description of polysaccharide solution rheology. This model is adapted to flow through porous media with

$$F_r - F_{r\infty} = (F_{r0} - F_{r\infty})[1 + (\lambda u)^2]^{(n-1)/2} \dots \dots \dots (4)$$

$$\text{and } \lambda = c_2(3 + 1/n)/\sqrt{k\phi}. \dots \dots \dots (5)$$

Fig. 2 shows curves generated with the Carreau model. These plots are based on viscosity data reported by Chauveteau<sup>10</sup> and Chauveteau and Zaitoun<sup>11</sup> for 200- and 2,400-ppm xanthan solutions. An important advantage of the Carreau model is that it avoids prediction of unrealistically low resistance factors at high fluid velocities. This feature is essential when predicting flow behavior in the vicinity of the wellbore in unfractured wells.

**Chauveteau Depletion-Layer Model.** Refs. 10 and 11 contend that steric hindrances cause fluid very near a solid surface to have a polymer concentration lower than that in a bulk solution. The low viscosity of this "depleted layer" reportedly can cause the apparent viscosity in porous media to appear to have a lower value than viscosity measured in a viscometer. To quantify this effect,  $F_{r0}$  in Eq. 4 is replaced by  $F_{rd}$ , where

$$F_{rd} = 1.77/[1 - (1 - 1.77/\mu_{rb})(1 - h_{dl}/r_t)^4]. \dots \dots \dots (6)$$

Here,  $h_{dl}$  is the thickness of the depletion layer, to which Chauveteau assigned a value of 0.3  $\mu\text{m}$ . The value 1.77 represents the apparent relative viscosity in the depleted layer. The apparent relative viscosity of fluid flowing in the center of a pore,  $\mu_{rb}$ , is assumed to be equal to the zero-shear-rate relative viscosity,  $F_{r0}$ . To be consistent with Refs. 10 and 11, the pore-throat radius,  $r_t$ , in consolidated porous media was estimated by

$$r_t = 1.75(2\sqrt{8k/\phi})^{0.65}. \dots \dots \dots (7)$$

This relation was found by use of sandstones with permeabilities from 3 to 365 md. The depletion-layer model (illustrated in Fig.

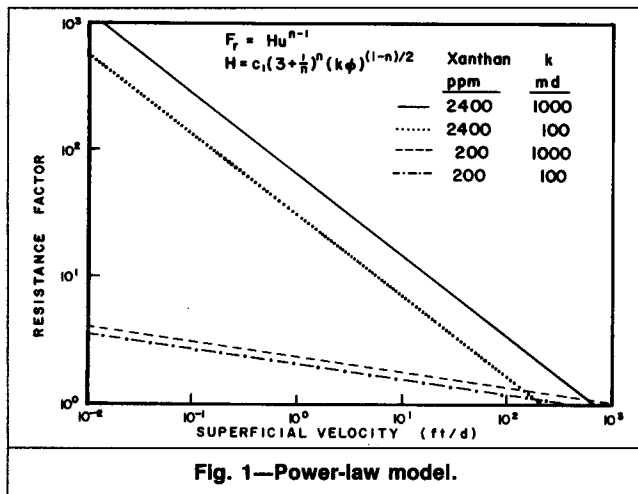


Fig. 1—Power-law model.

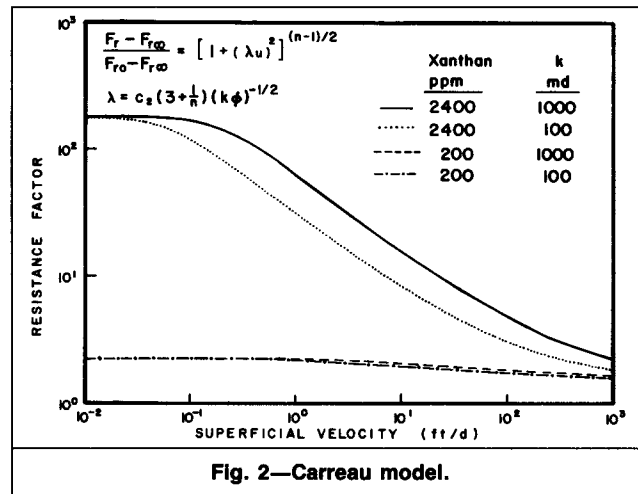


Fig. 2—Carreau model.

3 of Ref. 4) predicts decreasing zero-shear-rate resistance factors as permeability decreases.

**Cannella Model.** Cannella *et al.*<sup>9</sup> determined and correlated rheology for xanthan solutions in porous media (carbonates and sandstones with and without the presence of a residual oil saturation) over a wide range of conditions. Contrary to Refs. 10 and 11, they did not observe a strong influence of permeability on the power-law exponent,  $n$ , for xanthan solutions in porous media. Cannella *et al.* found the permeability dependence of xanthan rheology to be described quite well by

$$F_r = F_{r\infty} + (I/\mu_w)[(3n+1)/(4n)]^n (6u/\sqrt{k\phi})^{n-1} \dots (8)$$

The Cannella model is illustrated in Fig. 4 of Ref. 4. This model was applied successfully for superficial velocities between 0.005 and 3,000 ft/D and permeabilities between 47 and 740 md.<sup>9</sup> The principal difference from the Carreau model is noted at low fluid velocities. As fluid velocity decreases, resistance factors rise significantly above the value associated with the zero-shear viscosity for the fluid. Willhite and Uhl<sup>14</sup> and Hejri *et al.*<sup>15</sup> also observed this phenomenon.

**Willhite Empirical Power-Law Model.** Willhite and Uhl<sup>14</sup> and Hejri *et al.*<sup>15</sup> also determined and correlated rheology for xanthan solutions in porous media. Resistance factors from their correlations can be calculated with

$$F_r = k u^{n-1} / (\lambda_p \mu_w) \dots (9)$$

In Eq. 9,  $n$  and  $\lambda_p$  are empirical functions of permeability and can be found in Ref. 14 for flow of 500-, 1,000-, and 1,500-ppm xan-

than solutions through sandstones. The permeability dependence of the power-law exponent is weak; however, it is enough to skew the rheological curves (see Fig. 5 of Ref. 4).

Like the Cannella model, the Willhite model is based on rheology in porous media that was observed over a wide range of velocity and permeability. In Willhite and Uhl's<sup>14</sup> experiments, superficial velocities ranged from 0.02 to 23 ft/D and permeabilities ranged from 15.5 to 848 md. However, because the Willhite model is a power-law model, it predicts resistance factors that are less than unity at the high fluid velocities that commonly occur near a wellbore. To overcome this limitation, the Willhite model has been adapted to radial flow.\*

**Heemskerk Dual-Power-Law Model.** The models discussed to this point were developed to describe the rheology of shear-thinning solutions (notably xanthan solutions) in porous media. Solutions of synthetic polymers [notably partially hydrolyzed polyacrylamides (HPAM)] can exhibit both shear-thinning and shear-thickening behavior in porous media, depending on the fluid composition and velocity. Heemskerk *et al.*<sup>16</sup> used a dual-power-law model to describe the rheology of solutions that contain 1,000 ppm HPAM. The equations used in the model are identical to Eqs. 1 and 2 except that different sets of  $c_1$  and  $n$  values are used to yield Newtonian or shear-thinning rheology below the critical Deborah number,  $N_{De}$ , and to account for shear-thickening rheology above  $N_{De}$ . Here,

$$N_{De} = \Delta t_f \epsilon = \Delta t_f u / (\phi d_p) \dots (10)$$

$N_{De}$  is typically valued at unity, and it demarcates where elastic forces begin to dominate over viscous forces.  $\Delta t_f$  = characteristic

\*Personal communication with G.P. Willhite, U. of Kansas, Feb. 10, 1989.

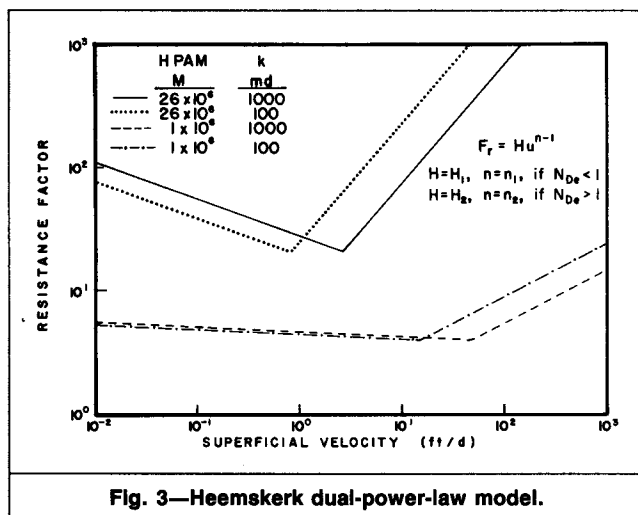


Fig. 3—Heemskerk dual-power-law model.

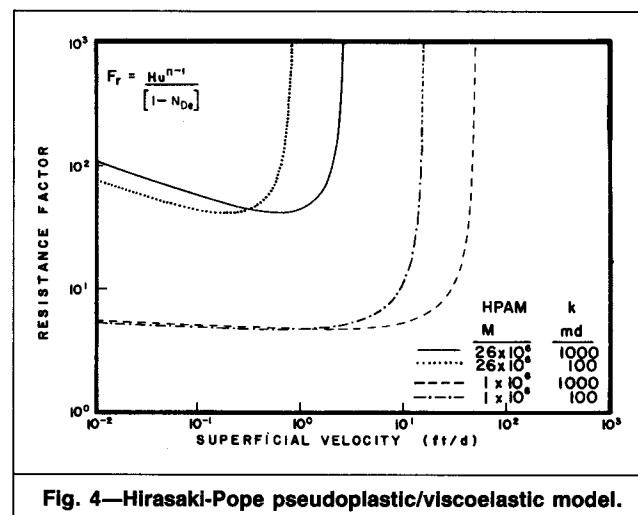


Fig. 4—Hirasaki-Pope pseudoplastic/viscoelastic model.

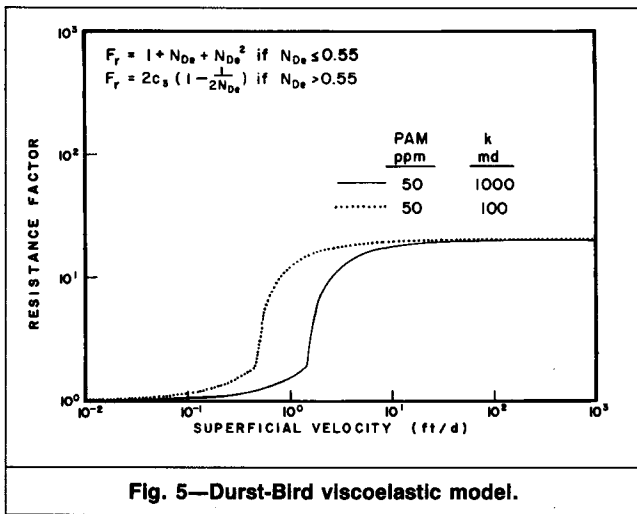


Fig. 5—Durst-Bird viscoelastic model.

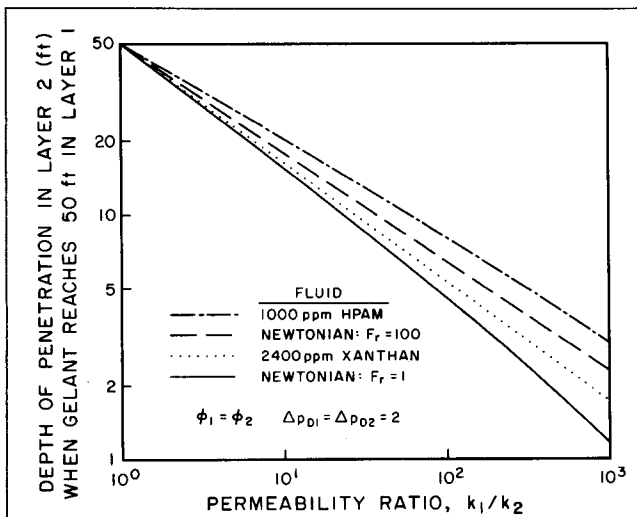


Fig. 6—Relative penetration of fluids in an unfractured injection well with multiple, noncommunicating layers.

relaxation time of the fluid and  $\epsilon$  = fluid strain rate. The average grain diameter,  $d_p$ , is given by

$$d_p = [(1 - \phi)/\phi] \sqrt{150k/\phi} \quad (11)$$

Fig. 3 shows the rheology in porous media predicted for 1,000 ppm HPAM solutions (with polymer molecular weights of 1 million and 26 million, respectively). The HPAM rheological data were taken from Ref. 16. The Heemskerk model was based on data obtained at superficial velocities from 0.1 to 60 ft/D and permeabilities from 486 to 11,650 md. Mechanical degradation limits the validity of this model at high fluid velocities.

**Hirasaki-Pope Pseudoplastic/Viscoelastic Model.** Hirasaki and Pope<sup>17</sup> proposed Eq. 12 to account for the dual pseudoplastic/viscoelastic behavior exhibited by HPAM solutions:

$$F_r = Hu^{n-1}/(1 - N_{De}) \quad (12)$$

Values for  $H$  and  $N_{De}$  are obtained with Eqs. 2 and 10, respectively. Fig. 4 shows the rheology predicted by this model. To allow a comparison with the Heemskerk model, values for  $n$ ,  $H$ , and  $N_{De}$  for HPAM solutions were again taken from Ref. 16.

The shear-thickening behavior predicted by the Hirasaki-Pope model is actually too steep to represent the rheology of HPAM solutions in porous media accurately. However, the model may still be of value in describing the behavior of fluids that exhibit shear-induced gelation.

TABLE 1—PARALLEL LINEAR COREFLOODS

Degree of penetration of gelling agent into 100-md core when gelling agent reaches the outlet of the 1,000-md core ( $L_{p2}/L_{p1}$ ). Core length = 1 ft, porosity = 0.2.

Fluid Model	$L_{p2}/L_{p1}$ for Given Pressure Drop in psi			
	1	10	100	1,000
Newtonian				
$F_r = 1$	0.100	0.100	0.100	0.100
$F_r = 10$	0.256	0.256	0.256	0.256
$F_r = 100$	0.309	0.309	0.309	0.309
$F_r = 1,000$	0.316	0.316	0.316	0.316
Shear Thinning				
Power law				
200 ppm xanthan	0.137	0.118	0.103	0.090*
2,400 ppm xanthan	0.316	0.295	0.098	0.058*
Carreau				
200 ppm xanthan	0.145	0.136	0.129	0.123
2,400 ppm xanthan	0.312	0.295	0.172	0.131
Chauveteau depletion layer				
200 ppm xanthan	0.143	0.135	0.128	0.122
2,400 ppm xanthan	0.210	0.137	0.124	0.122
Cannella				
200 ppm xanthan	0.173	0.159	0.147	0.138
2,400 ppm xanthan	0.316	0.297	0.174	0.132
Willhite empirical power law				
500 ppm xanthan	0.279	0.179	0.103	0.071*
1,500 ppm xanthan	0.582	0.384	0.118	0.062*
Shear Thickening				
Heemskerk dual power law				
HPAM, $M = 1$ million	0.201	0.194	0.236	0.274
HPAM, $M = 26$ million	0.299	0.300	0.311	0.315
Hirasaki-Pope				
HPAM, $M = 1$ million	0.205	0.103	0.316	0.316
HPAM, $M = 26$ million	0.087	0.316	0.316	0.316
Durst-Bird				
50 ppm HPAM	0.253	0.278	0.283	0.284

\*Resistance factors were < 1.

**Durst-Bird Viscoelastic Model.** Using concepts developed by Bird *et al.*<sup>18</sup>, Durst *et al.*<sup>19</sup> proposed a finitely extendable, nonlinear, elastic (FENE) dumbbell model to describe the rheology of dilute polyacrylamide (PAM) solutions. Resistance factors for this model can be calculated with

$$F_r = 1 + N_{De} + N_{De}^2, \text{ if } N_{De} \leq 0.55, \quad (13)$$

$$\text{and } F_r = 2c_3[1 - 1/(2N_{De})], \text{ if } N_{De} > 0.55. \quad (14)$$

Here,  $c_3$  is a constant related (in theory) to the number of statistical segments in a polymer chain. Fig. 5 illustrates the rheology predicted for a 50-ppm PAM solution.

The above discussion presents five models for describing the behavior of biopolymer solutions and three models characterizing synthetic polymer solutions. Clearly, not all the models can always be correct. Each model will have a range of conditions under which its application will be appropriate. For completeness, all the models are examined in the following analysis. While the models are based on experimental data, the reader should recognize that the performance of a given type of polymer will depend on a number of factors, including molecular weight, concentration, salinity, and temperature.

## Flow Systems and Numerical Treatment

**Flow Systems Considered.** Each rheological model was examined numerically using five two-layer systems. These systems included

**TABLE 2—FLOW RATIOS IN PARALLEL LINEAR CORES THAT ARE COMPLETELY FILLED WITH GELLING AGENT**

Flow ratio (in 100 md/1,000-md core).  
Core length = 1 ft, porosity = 0.2.

Fluid Model	Flow Ratio for Given Pressure Drop in psi			
	1	10	100	1,000
Newtonian				
$F_r = 1$	0.100	0.100	0.100	0.100
$F_r = 10$	0.100	0.100	0.100	0.100
$F_r = 100$	0.100	0.100	0.100	0.100
$F_r = 1,000$	0.100	0.100	0.100	0.100
Shear Thinning				
Power law				
200 ppm xanthan	0.085	0.085	0.085	0.085*
2,400 ppm xanthan	0.013	0.013	0.013	0.013*
Carreau				
200 ppm xanthan	0.098	0.094	0.095	0.096
2,400 ppm xanthan	0.099	0.039	0.034	0.079
Chauveteau depletion layer				
200 ppm xanthan	0.101	0.097	0.097	0.098
2,400 ppm xanthan	0.112	0.101	0.100	0.100
Cannella				
200 ppm xanthan	0.090	0.091	0.092	0.093
2,400 ppm xanthan	0.013	0.014	0.033	0.078
Willhite empirical power law				
500 ppm xanthan	0.079	0.085	0.091	0.098*
1,500 ppm xanthan	0.231	0.101	0.044	0.019*
Shear Thickening				
Høemskerk dual power law				
HPAM, $M = 1$ million	0.095	0.095	0.141	0.141
HPAM, $M = 26$ million	0.061	0.070	0.176	0.176
Hirasaki-Pope				
HPAM, $M = 1$ million	0.097	0.027	0.316	0.316
HPAM, $M = 26$ million	0.003	0.316	0.316	0.316
Durst-Bird				
50 ppm HPAM	0.232	0.164	0.109	0.101

\*Resistance factors were < 1.

**TABLE 3—PARALLEL RADIAL COREFLOODS**

Degree of penetration of gelling agent into 100-md core when gelling agent reaches the outer radius of 1,000-md core.  $\phi = 0.2$ ,  $r_{p1} = 50$  ft,  $r_w = 0.5$  ft.

Fluid Model	$(r_{p2} - r_w)/(r_{p1} - r_w)$ For Given Pressure Drop in psi		
	50	500	5,000
Newtonian			
$F_r = 1$	0.309	0.309	0.309
$F_r = 10$	0.352	0.352	0.352
$F_r = 100$	0.357	0.357	0.357
$F_r = 1,000$	0.358	0.358	0.358
Shear Thinning			
Power law			
200 ppm xanthan	0.321	0.312*	0.301*
2,400 ppm xanthan	0.326	0.324*	0.249*
Carreau			
200 ppm xanthan	0.329	0.326	0.324
2,400 ppm xanthan	0.339	0.326	0.325
Chauveteau depletion layer			
200 ppm xanthan	0.332	0.329	0.326
2,400 ppm xanthan	0.392	0.338	0.327
Cannella			
200 ppm xanthan	0.335	0.332	0.330
2,400 ppm xanthan	0.326	0.326	0.325
Willhite empirical power law			
500 ppm xanthan	0.382	0.367*	0.316*
1,500 ppm xanthan	0.591	0.444*	0.287*
Shear Thickening			
Høemskerk dual power law			
HPAM, $M = 1$ million	0.343	0.365	0.379
HPAM, $M = 26$ million	0.344	0.410	0.417
Hirasaki-Pope			
HPAM, $M = 1$ million	0.360	0.558	0.558
HPAM, $M = 26$ million	0.388	0.558	0.558
Durst-Bird			
50 ppm HPAM	0.384	0.360	0.356

\*Resistance factors were < 1.

(1) parallel linear corefloods, (2) parallel radial corefloods, (3) an unfractured injection well with  $\Delta p_{D1} = \Delta p_{D2} = 2$  (corresponding to a case where Layer 1 is watered-out and Layer 2 contains a light oil such that the water/oil mobility ratio is unity), (4) an unfractured injection well with  $\Delta p_{D1} = 2$  and  $\Delta p_{D2} = 50$  (corresponding to a case where Layer 1 is watered-out and Layer 2 contains a viscous oil such that the water/oil mobility ratio is about 40), and (5) a vertically fractured injection well with  $\Delta p_{D1} = \Delta p_{D2} = 10$ . ( $\Delta p_D$  is explained in Refs. 1 and 4.) In each system, the permeability of Layer 1 was 1,000 md, while the permeability of Layer 2 was 100 md. Porosity was 0.2 in all layers. Crossflow between layers was not allowed.

In each flow system, the aqueous gelant was injected simultaneously into the two layers through a shared injector, and fluids were produced through a shared producer. Displacement of water by the gelant was assumed to be piston-like, fluids were incompressible, dispersion and chemical retention were neglected, and flow was horizontal. Pressure drop was maintained constant between the injector and the producer. In the corefloods, no mobile oil was present. In the unfractured wells, no mobile oil existed within a radius of 50 ft from the injector. Similarly, in the vertically fractured injector, no mobile oil existed within 50 ft from the fracture face.

**Degree of Penetration.** The degree of penetration,  $L_{p2}/L_{p1}$  or  $(r_{p2} - r_w)/(r_{p1} - r_w)$ , indicates the fractional distance or radius that the gelant penetrates into Layer 2 when the gelant reaches a predetermined distance,  $L_{p1}$ , or radius,  $r_{p1}$ , in Layer 1. In the corefloods, the gelant was allowed to reach the outlet of the most

permeable core. The core length for the linear corefloods was 1 ft (so  $L_{p1} = 1$  ft). For the parallel radial corefloods, the inner core radius,  $r_w$ , was 0.5 ft, while the outer core radius was 50 ft (so  $r_{p1} = 50$  ft).

To date, most gel treatments have used small volumes of gelant formulation. Typically, the gelant penetrates only 50 to 100 ft into the most permeable rock matrix. Therefore, in the unfractured injection wells, the gelant was allowed to penetrate to a radius of 50 ft from the wellbore in Layer 1, so again,  $r_{p1} = 50$  ft and  $r_w = 0.5$  ft. In the vertically fractured well, the gelant penetrated linearly 50 ft from the fracture face in Layer 1, so  $L_{p1} = 50$  ft.

**Numerical Procedures.** For each combination of flow system and rheological model, numerical methods were used to calculate the degree of penetration, fluid velocity, and resistance factor in both layers as a function of volume of gelant injected. A modified Euler method combined with the Secant method<sup>20</sup> was used to determine the degree of penetration for a given system. With Newtonian fluids with resistance factors ranging from 1 to 1,000, results from the numerical calculations were found to agree well with analytical solutions for each of the five flow systems. Tests of gridblock and timestep sizes were performed to confirm that the numerical results were insensitive to these variables under the conditions examined.

## Results

**Parallel Linear Corefloods.** Table 1 summarizes the degree-of-penetration calculations for parallel linear corefloods. The Newto-

nian fluids set the standard for comparison. A Newtonian fluid with  $F_r=1$  generally provides the lowest degree of penetration into the less permeable core, yielding a value of 0.1 for the 100/1,000-md parallel corefloods. In contrast, the degree of penetration is 0.316 for displacement of water with the Newtonian fluid with  $F_r=1,000$ . This 0.316 value is near the theoretical limit of  $(k_2/k_1)^{1/2}$  for injection of a Newtonian fluid with an infinite viscosity (see Eq. 1 of Ref. 1).

The degree of penetration is independent of pressure gradient for Newtonian fluids. However, the behavior of non-Newtonian fluids can be very dependent on the applied pressure drop. Table 1 illustrates this for pressure drops between 1 and 1,000 psi.

Much of the behavior of the various fluids can be rationalized by following a simple rule: the more viscous the gelant, the greater the degree of penetration into the less permeable layer.

Note in Table 1 that the concentrated polymer solutions generally penetrate into the less permeable layer to a greater degree than dilute polymer solutions. Also, for the shear-thinning fluids, the degree of penetration decreases with increased pressure drop. This result occurs largely because the shear-thinning fluids are less viscous at the high velocities associated with high pressure drops. Similar logic rationalizes the increased degree of penetration with increased pressure drop for shear-thickening fluids. The results suggest that to some degree, shear-thinning fluids may be preferred over shear-thickening fluids if high injection rates can be maintained during gel placement. The converse would apply if injection rates must be low.

The starred entries in Tables 1 through 3 denote situations where resistance factors were less than unity during part or all of the flood. In several cases, these entries appear to indicate that the polymeric fluid provided a lesser degree of penetration than the water-like fluid ( $F_r=1$ ). However, the starred entries are not meaningful, for two reasons. First, no known aqueous fluid exhibits a resistance factor less than unity in porous media. The power-law models' predictions of resistance factors less than unity simply represent a deficiency in the models. Second, if the resistance factors were truly less than unity, then viscous fingering would play an important role in determining the degree of penetration. Because viscous fingering was not incorporated into the calculations, the predictions are not valid for the starred entries.

Except for the starred entries, only two entries in Table 1 are less than the value associated with a water-like fluid. One entry is for the power-law model for a 2,400-ppm xanthan solution during injection with a 100-psi pressure drop. This entry is only 2% less than that for a water-like fluid. To understand why this entry is  $<0.1$ , refer to Fig. 1. For 100 psi/ft, the fluid velocity averages around 600 ft/D in the 1,000-md core, so the resistance factor is very close to unity (actually ranging from 1.04 to 1.12 during the flood). In the 100-md core, however, the velocity averages around 60 ft/D and the resistance factor averages about 2.3. The higher resistance factor in the 100-md core is enough to maintain the degree of penetration slightly below 0.1. Note, however, that the degree of penetration is significantly greater than 0.1 for pressure drops of 1 and 10 psi, where lower fluid velocities and much higher resistance factors occur in both cores.

The other value  $<0.1$  in Table 1 is associated with the Hirasaki-Pope model for the HPAM with  $M=26$  million during injection at 1 psi/ft. This entry is 13% less than that for a water-like fluid. To understand this value, refer to Fig. 4. For 1 psi/ft, the fluid velocity in the 100-md core averages 0.2 ft/D and the average resistance factor is 43. In contrast, the average velocity in the 1,000-md core is 2.6 ft/D, yielding an average resistance factor of five. The degree of penetration of 0.087 results because the resistance factor in the 100-md core is more than eight times that in the 1,000-md core. Note that for higher pressure drops, high degrees of penetration are observed in the 100-md core. Thus, non-Newtonian rheology can be exploited to reduce the degree of penetration, but only under a very limited set of conditions.

Careful consideration of Figs. 1 through 5 reveals that alteration of the permeability dependence of fluid rheology could influence the degree of penetration. In seven of the eight models, the apparent shear rate in porous media has been modeled as being propor-

tional to permeability to the  $-0.5$  power.<sup>8-11,16-19</sup> For shear-thinning fluids, the degree of penetration into low-permeability zones would be reduced if the permeability exponent was  $>-0.5$ . For shear-thickening fluids, the degree of penetration would be reduced if the permeability exponent was  $<-0.5$ . Of course, altering the permeability dependence of fluid rheology could be difficult.

**Use of Flow Ratios To Assess Selective Placement.** Chang *et al.*<sup>21</sup> considered flow ratios in parallel bundles of capillary tubes. Flow ratio was defined as the flow rate in one bundle of capillaries (or porous medium) divided by the flow rate in a parallel bundle of capillaries. Both capillary bundles were the same length, were completely filled with the same fluid, and were exposed to the same pressure drop under steady-state conditions. Chang *et al.* noted that for shear-thinning fluids, a greater fraction of the fluid flowed through the more permeable bundle than would be expected from the permeability ratio for the two bundles. In other words, one capillary bundle might be 10 times more permeable than another, thus allowing the flow ratio for water to be 10:1. During steady-state injection of a power-law fluid that had a power-law exponent of 0.5, however, the flow ratio would be 32:1. This led Chang *et al.* to conclude that shear-thinning xanthan solutions would be more selective than water in preferentially entering high-permeability zones during gel placement without zone isolation.

Chang *et al.*'s argument would be valid if all layers in a reservoir were filled completely with only xanthan solution. During gel placement in reservoirs, however, gelants displace reservoir fluids (primarily water for injection-well treatments). In that case, the above conclusion is usually incorrect, as the results in Tables 1 through 3 demonstrate. A detailed analysis of injection profiles from a field project<sup>21</sup> confirms this.<sup>22</sup>

Table 2 lists flow ratios (flow rate in the 100-md core relative to that in the 1,000-md core) for parallel cores completely filled with a single fluid. Each flow ratio in Table 2 can be compared with the corresponding degree of penetration from a displacement study in Table 1. Many of the listings in Table 2 are dramatically lower than the corresponding listings in Table 1. Thus, flow ratios from parallel cores completely filled with a single fluid should not be used to assess the selectivity of a gelant.

**Parallel Radial Corefloods.** Table 3 summarizes the degree-of-penetration calculations for parallel radial corefloods. For a given rheological model, the degree of penetration in parallel radial corefloods is generally significantly greater than that in parallel linear corefloods. This observation was reported earlier for Newtonian fluids.<sup>1</sup>

In Table 3, the starred entries are associated with power-law fluids in which resistance factors were less than unity. For the reasons mentioned earlier, these values should be viewed with caution.

Except for three of the starred values, no entry in Table 3 lists a degree of penetration that is less than that for a water-like fluid ( $F_r=1$ ). Most values are 0.309 to 0.400. Note that the variation of values for degree of penetration is much less for the radial systems than for the linear systems. This difference occurs primarily because the degree of penetration in radial flow is proportional to the square root of the volume of injected fluid. If an effect changes the volume of injected fluid in a zone by a certain factor, then the degree of penetration will be changed by roughly the square root of that factor. The degree of penetration is more sensitive in linear flow because it varies linearly with the volume of fluid injected. A secondary factor is that the wide range of velocities experienced in radial flow mitigates the impact of abrupt rheological changes.

**Fractured and Unfractured Injection Wells.** Results for injection wells (both fractured and unfractured) are listed in Tables 3A, 3B, and 4 of Ref. 4. Examination of these tables reveals that none of the models predict a degree of penetration in the less permeable layer that is less than the value provided by a water-like fluid (except some cases where  $F_r < 1$ ). The results for the unfractured wells closely follow the trends exhibited during the radial corefloods (Table 3). Similarly, the behavior observed for the vertically fractured well follows that noted for the linear corefloods (Table 1).

A previous study<sup>1</sup> found that the need for zone isolation during gel placement in unfractured wells is much greater than in fractured wells. Because this conclusion was based on injection of a water-like gelant ( $F_r=1$ ) and because a water-like gelant generally will provide the least degree of penetration into less permeable zones, this conclusion is also valid for gelants having the rheological properties discussed above.

For the displacement calculations described above, the gelant penetrated a fixed distance (50 ft) into the 1,000-md layer. Similar calculations have been performed in which the depth of penetration in the 1,000-md layer,  $r_{p1}$ , was varied. These calculations reveal that the degree of penetration of gelant in the 100-md layer,  $(r_{p2}-r_w)/(r_{p1}-r_w)$ , is insensitive to  $r_{p1}$  for  $r_{p1}$  values between 25 and 400 ft.

**Other Permeability Ratios.** Although this work focused on systems with a 10:1 permeability ratio, the trends and conclusions are applicable to other permeability ratios. Fig. 6 shows depth-of-penetration calculations as a function of permeability ratio for two Newtonian fluids ( $F_r=1$  and  $F_r=100$ ) and for two non-Newtonian fluids. The two non-Newtonian fluids include the 2,400-ppm xanthan solution from the Carreau model (Fig. 2) and the 1,000-ppm HPAM ( $M=26$  million) solution from the Heemskerck model (Fig. 3). In generating Fig. 6, the pressure drop between the injector and the producer was 500 psi and  $k_2$  was 100 md. When  $k_1$  is fixed at 1,000 md, a plot is generated that is virtually the same as Fig. 6. Note that for a given permeability ratio, the three viscous fluids penetrate to a greater depth in the less permeable layer than the water-like fluid.

### Other Rheological Considerations

A permeability dependence beyond that described in Figs. 1 through 5 has been reported for resistance factors of aqueous polymer solutions.<sup>23,24</sup> As permeability decreases, resistance factors and residual resistance factors can increase dramatically. This increase can be attributed to constriction of flow paths by retained polymer.<sup>25</sup> An increase in resistance factor and chemical retention with decreasing permeability will decrease the depth of penetration of gelants into less permeable rock. However, a large decrease in permeability often accompanies these effects.<sup>23,24</sup> Analyses conducted with the available experimental data suggest that these phenomena usually will not improve the effectiveness of gel treatments.<sup>1,4,22,26</sup>

In the above analyses, the rheology during the process of gel placement was assumed to be that of polymer solutions without any crosslinker. Is this assumption valid? The answer depends on how early in the gelation process the gelants are injected. For at least two gelants (resorcinol/formaldehyde and  $Cr^{3+}$ /xanthan), the rheology in porous media can be unaffected by the crosslinker for a large fraction of the time before gelation.<sup>22,26</sup> Thus, the assumption can be valid if the gel-placement process is completed before the gelation reaction proceeds too far.

If injection is still occurring at the time that gel aggregates approach the size of pore throats, then significant changes in rheology may be observed.<sup>27,28</sup> Whether these changes are beneficial or harmful remains to be established. If they impair gel placement, flow of gel aggregates could be avoided by controlling gelation times, injection rates, and shut-in times. On the other hand, if flow of gel aggregates is beneficial, then gelation times and injection rates could be manipulated for a positive effect.

During brine injection after gelation, residual resistance factors (brine mobility before gel placement divided by brine mobility after gel placement) may depend on injection rates.<sup>22,26</sup> In particular, an apparent shear-thinning behavior has been observed. For resorcinol/formaldehyde and  $Cr^{3+}$ /xanthan gels, analysis of experimental results indicates that this apparent shear-thinning behavior will not eliminate the need for zone isolation during gel placement in unfractured injection wells. The search continues for gel systems and properties that can be exploited to optimize gel placement.

### Conclusions

1. Except in rare cases, non-Newtonian rheology of existing polymeric gelants will not reduce the degree of penetration into low-SPE Reservoir Engineering, May 1991

permeability zones below the value that is achievable with water-like gelants (i.e., where  $F_r=1$ ).

2. Compared with water-like gelants, currently available non-Newtonian gelants (e.g., those containing xanthan or HPAM) will not reduce the need for zone isolation during gel placement in radial-flow systems.

3. Steady-state flow ratios from parallel cores underestimate the ability of gelants to penetrate into low-permeability strata.

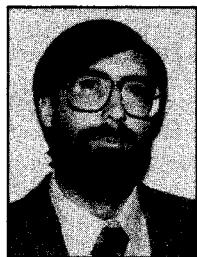
### Nomenclature

- $c_1$  = constant in Eq. 2
- $c_2$  = constant in Eq. 5
- $c_3$  = constant in Eq. 14
- $d_p$  = average grain diameter (see Eq. 11), ft [m]
- $F_r$  = resistance factor (water mobility divided by mobility of gelant)
- $F_{rd}$  = resistance factor given by Eq. 6
- $F_{r0}$  = resistance factor at zero fluid velocity
- $F_{r\infty}$  = resistance factor at infinite fluid velocity
- $h_{dl}$  = depletion-layer thickness,  $\mu\text{m}$
- $H$  = given by Eq. 2
- $I$  = consistency index from viscosity vs. shear rate data
- $k_i$  = effective permeability to water in Layer  $i$ , md
- $L_{pi}$  = distance gelant has propagated in linear core or from vertical fracture face (into rock matrix) in Layer  $i$ , ft [m]
- $L_{pmax}$  = maximum distance gelant will propagate from fracture face in most-permeable layer, ft [m]
- $M$  = molecular weight
- $n_s$  = power-law exponent
- $N_{De}$  = Deborah number (see Eq. 10)
- $\Delta P_{Di}$  = pressure drop between  $r_{pmax}$  (or  $L_{pmax}$ ) and production well divided by pressure drop between injection well and  $r_{pmax}$  (or  $L_{pmax}$ ) in Layer  $i$  before gel placement
- $r_{pi}$  = gelant's radius of penetration in Layer  $i$ , ft [m]
- $r_{pmax}$  = gelant's maximum radius of penetration in most permeable layer, ft [m]
- $r_t$  = pore-throat radius,  $\mu\text{m}$
- $r_w$  = wellbore radius, ft [m]
- $\Delta t_f$  = fluid relaxation time, seconds
- $u$  = fluid flux or superficial velocity, ft/D [m/s]
- $\epsilon$  = fluid strain rate, seconds<sup>-1</sup>
- $\lambda$  = given by Eq. 5
- $\lambda_p$  = empirical function in Eq. 9
- $\mu_{rb}$  = apparent relative viscosity in center of pore
- $\mu_w$  = water viscosity, cp
- $\phi_i$  = effective aqueous-phase porosity in Layer  $i$

### References

1. Seright, R.S.: "Placement of Gels To Modify Injection Profiles," paper SPE 17332 presented at the 1988 SPE/DOE Enhanced Oil Recovery Symposium, Tulsa, April 17-20.
2. Seright, R.S.: "Impact of Dispersion on Gel Placement for Profile Control," paper SPE 20127 presented at the 1990 SPE Permian Basin Oil and Gas Recovery Conference, Midland, March 8-9.
3. Liang, J., Lee, R.L., and Seright, R.S.: "Placement of Gels in Production Wells," paper SPE 20211 presented at the 1990 SPE/DOE Enhanced Oil Recovery Symposium, Tulsa, April 22-25.
4. Seright, R.S.: "Effect of Rheology on Gel Placement," paper SPE 18502 presented at the 1989 SPE Intl. Symposium on Oilfield Chemistry, Houston, Feb. 8-10.
5. Bird, R.B., Stewart, W.E., and Lightfoot, E.N.: *Transport Phenomena*, John Wiley & Sons Inc., New York City (1960) 197-207.
6. Christopher, R.H. and Middleman, S.: "Power-Law Flow Through a Packed Tube," *Ind. & Eng. Chem. Fund.* (Nov. 1965) 4, No. 4, 422-26.
7. Gogarty, W.B., Levy, G.L., and Fox, V.G.: "Viscoelastic Effects in Polymer Flow Through Porous Media," paper SPE 4025 presented at the 1972 SPE Annual Fall Meeting, San Antonio, Oct. 8-11.
8. Teeuw, D. and Hesselink, F.T.: "Power-Law Flow and Hydrodynamic Behavior of Biopolymer Solutions in Porous Media," paper SPE 8982

## Author



**Randy Seright is a senior engineer in charge of improved waterflooding and chemical flooding processes at the New Mexico Petroleum Recovery Research Center in Socorro. Previously, he worked for Exxon Production Research Co. He holds a PhD degree in chemical engineering from the U. of Wisconsin. Seright is a member of the Program Committee for the 1991 SPE Oilfield Chemistry Symposium and serves on the Editorial Review Committee.**

- presented at the 1980 SPE Intl. Symposium on Oilfield and Geothermal Chemistry, Stanford, CA, May 28-30.
9. Cannella, W.J., Huh, C., and Seright, R.S.: "Prediction of Xanthan Rheology in Porous Media," paper SPE 18089 presented at the 1988 SPE Annual Technical Conference and Exhibition, Houston, Oct. 2-5.
  10. Chauveteau, G.: "Rodlike Polymer Solution Flow Through Fine Pores: Influence of Pore Size on Rheological Behavior," *J. Rheology* (1982) 26, No. 2, 111-42.
  11. Chauveteau, G. and Zaitoun, A.: "Basic Rheological Behavior of Xanthan Polysaccharide Solutions in Porous Media: Effects of Pore Size and Polymer Concentration," *Proc., European Symposium on Enhanced Oil Recovery*, F.J. Fayers (ed.), Bournemouth, U.K. (1981) 197-212.
  12. Duda, J.L., Hong, S., and Klaus, E.E.: "Flow of Polymer Solutions in Porous Media: Inadequacy of the Capillary Model," *Ind. & Eng. Chem. Fund.* (1983) 22, 299-305.
  13. Bird, R.B., Armstrong, R.C., and Hassager, O.: *Dynamics of Polymeric Liquids*, John Wiley & Sons, New York City (1977) 1, 210-11.
  14. Willhite, G.P. and Uhl, J.T.: "Correlation of the Flow of Flocon 4800 Biopolymer With Polymer Concentration and Rock Properties in Berea Sandstone," *Water-Soluble Polymers for Petroleum Recovery*, G.A. Stahl and D.N. Schulz (eds.), Plenum Press, New York City (1988) 101-19.
  15. Hejri, S., Willhite, G.P., and Green, D.W.: "Development of Correlations To Predict Flocon 4800 Biopolymer Mobility in Porous Media," paper SPE 17396 presented at the 1988 SPE/DOE Enhanced Oil Recovery Symposium, Tulsa, April 17-20.
  16. Heemskerk, J. et al.: "Quantification of Viscoelastic Effects of Polyacrylamide Solutions," paper SPE 12652 presented at the 1984 SPE/DOE Symposium on Enhanced Oil Recovery, Tulsa, April 15-18.
  17. Hirasaki, G.J. and Pope, G.A.: "Analysis of Factors Influencing Mobility and Adsorption in the Flow of Polymer Solution Through Porous Media," *SPEJ* (Aug. 1974) 337-46.
  18. Bird, R.B. et al.: *Dynamics of Polymeric Liquids*, John Wiley & Sons, New York City (1977) 2, 495-507.
  19. Durst, F., Hass, R., and Interthal, W.: "Laminar and Turbulent Flows of Dilute Polymer Solutions: A Physical Model," *Rheologica Acta* (1982) 21, No. 4-5, 572-77.
  20. Burden, R.L. and Faires, J.D.: *Numerical Analysis*, third edition, Prindle, Weber & Schmidt, Boston (1985) 46-48, 199-225.
  21. Chang, P.W. et al.: "Selective Emplacement of Xanthan/Cr(III) Gels in Porous Media," paper SPE 17589 presented at the 1988 SPE Intl. Meeting on Petroleum Engineering, Tianjin, Nov. 1-4.
  22. Seright, R.S. and Martin, F.D.: "Fluid Diversion and Sweep Improvement With Chemical Gels in Oil Recovery Processes," first annual report, No. 90-19, New Mexico Petroleum Recovery Research Center, Socorro (May 1990).
  23. Vela, S., Peaceman, D.W., and Sandvik, E.I.: "Evaluation of Polymer Flooding in a Layered Reservoir With Crossflow, Retention, and Degradation," *SPEJ* (April 1976) 82-96.
  24. Jennings, R.R., Rogers, J.H., and West, T.J.: "Factors Influencing Mobility Control By Polymer Solutions," *JPT* (March 1971) 391-401.
  25. Zaitoun, A. and Kohler, N.: "The Role of Adsorption in Polymer Propagation Through Reservoir Rocks," paper SPE 16274 presented at the 1987 SPE Intl. Symposium on Oilfield Chemistry, San Antonio, Oct. 4-6.
  26. Seright, R.S. and Martin, F.D.: "Impact of Gelation pH, Rock Permeability, and Lithology on the Performance of a Monomer-Based Gel," paper SPE 20999 presented at the 1991 SPE Intl. Symposium on Oilfield Chemistry, Anaheim, Feb. 20-22.
  27. McCool, C.S., Green, D.W., and Willhite, G.P.: "Permeability Reduction Mechanisms Involved in In-Situ Gelation of a Polyacrylamide/Chromium(VI)/Thiourea System," *SPEJ* (Feb. 1991) 77-83.
  28. Hejri, S., Green, D.W., and Willhite, G.P.: "In-Situ Gelation of a Xanthan/Cr(III) Gel System in Porous Media," paper SPE 19634 presented at the 1989 SPE Annual Technical Conference and Exhibition, San Antonio, Oct. 8-11.

## SI Metric Conversion Factors

cp × 1.0*	E-03 = Pa·s
ft × 3.048*	E-01 = m
md × 9.869 233	E-04 = μm <sup>2</sup>
psi × 6.894 757	E+00 = kPa

\*Conversion factor is exact.

**SPEJ**

Original SPE manuscript received for review Feb. 8, 1989. Paper accepted for publication Nov. 26, 1990. Revised manuscript received Aug. 23, 1990. Paper (SPE 18502) first presented at the 1989 SPE Intl. Symposium on Oilfield Chemistry held in Houston, Feb. 8-10.